IMPROVEMENT OF EARTHQUAKE EPICENTRAL LOCATIONS USING T-PHASES: TESTING BY COMPARISON WITH SURFACE WAVE RELATIVE EVENT LOCATIONS

Donald W. Forsyth, Yingjie Yang

Brown University

Sponsored by The Defense Threat Reduction Agency

Contract No. DTRA 01-00-C-0071

ABSTRACT

A deployment of 51 ocean-bottom seismometers (OBS) on the seafloor spanning 800 km across the East Pacific Rise provides a unique opportunity to test the robustness of epicentral location techniques using T-phases. A standard technique for locating events with T-phases is to pick the arrival the time of peak energy, then proceed as if it were an unscattered phase originating at the epicenter. Such an approach has been shown to have no apparent bias in epicentral location. Comparison of waveforms at nearby stations, however, shows that peak energy arrival time can shift to different parts of the wavetrain due to incoherent interference between waves excited or scattered from different locations, even for stations only a few kilometers apart, forcing operator identification of particular features in the waveform. At greater sensor separations, such identification cannot be performed with confidence. We show that a 75% reduction in variance relative to picks of peak arrival times can be achieved by fitting an assumed functional shape to the entire envelope of the T-phase. Since most of the variation in the envelope is caused by scattering and interference of the waves, "noise" is proportional to signal and is log-normal. Best results are obtained by fitting the log of the envelope, which transforms the noise into a nearly constant, Gaussian distributed background and de-emphasizes individual peaks. By fitting the entire long wavetrain of the T-phase, excitation by individual bathymetric features is also de-emphasized.

We test the stability of this approach for events of greatly different size using a mainshock/aftershock sequence of earthquakes at the northern end of the Easter microplate. In addition, for the larger earthquakes, we can compare relative event locations with those determined by cross-correlating waveforms of Rayleigh and Love surface waves recorded teleseismically. The T-phases from the OBSs are supplemented by T-phases recorded at GSN station RPN. Relative event locations show that there is no apparent bias in T-phase locations, as the 95% confidence intervals of locations from the two approaches overlap. Error ellipses are smaller for surface waves than for T-phases, but the T-phase location and detection can be extended to much smaller events.

KEY WORDS: hydroacoustic methods, earthquake location, surface waves, ocean-bottom seismometers

OBJECTIVES

The objectives of this research are

- To explore the synergy between hydroacoustic and seismic techniques for detecting, locating and discriminating between earthquakes and explosions using an array of ocean-bottom instruments,
- To characterize velocity, scattering and attenuation characteristics of T-phases and long- and short-period surface waves in young seafloor in the Pacific using seismograms recorded at an array of OBSs and hydrophones in the MELT Experiment,
- To characterize the excitation characteristics of typical events in the eastern Pacific, including nuclear tests in French Polynesia, based on these ocean-bottom recordings,
- To develop procedures for locating events using a combination of T-phases and surface waves, and
- To develop models for the excitation and scattering of short-period surface waves.

RESEARCH ACCOMPLISHED

The MELT Experiment in 1995/96 (Figure 1) provides a unique opportunity to study the lateral variability of hydroacoustic phases recorded on the seafloor. With such an understanding, we should be able to improve the picking of arrival times for determination of epicenters. The many stations of the array (recording pressure and in many cases three components of displacement) provide redundancy both in terms of location and a variety of paths to assess repeatability of waveforms. Here we focus on a particular earthquake sequence in relatively uniform water depths as a control test. The precision of location is tested by comparing locations from T-phases with relative event locations using surface waves recorded at teleseismic stations, a completely independent data set.

A quick examination of the smoothed envelopes of T-phases from a strike-slip event at the northern end of the Easter microplate recorded at some of the stations of the array illustrates the great variability in waveforms, even at nearby stations (Figure 2). One traditional way of picking arrival times is to pick the peak energy arrival. Closely spaced stations S14 and S16 in figure 2 both have clear, narrow, peak arrivals. The time difference between arrival times, however, is too great to be consistent with a single direct wave traveling to stations whose epicentral distances differ by less than 3 km (the stations are about 10 km apart). Total epicentral distance is on the order of 600 km. The envelopes at other closely spaced station pairs have even less resemblance. This great variability in waveform probably stems from interference of multiple waves traveling from multiple points of excitation or transmission on the seafloor near the source, effectively creating signal-generated noise in the wave shapes.

If the noise in the envelope shape is signal generated, then it should increase in amplitude with increasing amplitude of the signal and it should be approximately log-normal distributed. Figure 3 demonstrates that this is the case; for a typical station, after taking the log of the envelope, noise is approximately constant throughout the record, including background noise. There is an overall gradual growth in amplitude of the log of the envelope, followed by an even slower gradual decay. Specific peaks in amplitude of the envelope correspond to fortuitous constructive interference between waves and should not be assigned any great significance, i.e., should not be viewed as characteristic times to be picked in locating the event (the caveat is that we are looking at events recorded at depths of 3 km or more and thus the hydroacoustic phases are not dominated by fundamental mode propagation in the SOFAR channel). When viewed in log-space, the individual peaks in amplitude appear as nothing more than minor noise fluctuations on the overall pattern of growth and decay of the envelope.

The overall, approximately linear growth and decay of the log of the envelope suggests fitting the signal with an empirical function of exponential growth followed by exponential decay. We are experimenting with other, more complex functional forms that describe the shape somewhat better and are working toward evaluating shapes based on models of the excitation and propagation, but for now we concentrate on the results obtainable with a very simple model that provides a good empirical fit. The envelope is thus described by background noise plus exponential growth followed by exponential decay with a different time constant. Amplitude of envelope, $A_E(t)$, as function of time is given by

$t \geq t_o$

$$A_E = \left[A_0^2 + A_1^2 \exp\left(\frac{-2\{t_0 - t\}}{t_a} \right) \right]^{\frac{1}{2}}$$

$t > t_o$

$$A_E = \left[A_0^2 + A_1^2 \exp\left(\frac{-2\{t - t_0\}}{t_b} \right) \right]^{\frac{1}{2}}$$

where A_o is the amplitude of background noise, A_1 is the maximum amplitude of the signal, t_o is the characteristic arrival time, t_a is the characteristic growth time, and t_b is the characteristic decay time. An additional factor would have to be added for large earthquakes with long-duration sources, but the largest earthquake in this study is m_b ~4.5, for which the source duration is negligible compared to the duration of the hydroacoustic signal.

Thus, instead of basing the pick of the arrival time on a particular peak amplitude which may depend on highly variable wave interference or excitation from a single bathymetric feature, we base it on the overall shape of the signal, identifying the peak of the model shape as the arrival time after optimizing amplitudes and growth and decay times. The least squares fitting of the function is performed to the log of the envelope so that residuals or errors are approximately normally distributed, and undue emphasis is not placed on trying to match an individual peak in amplitude caused by random, constructive interference.

One way to judge the quality of the arrival time picks is to examine the variance of the travel-time residuals. Within the array, travel times are a linear function of epicentral distance (Figure 4) and the residuals from a linear fit are equivalent to travel-time residuals. Arrival times based on the peak of the model function yield a reduction of variance of more than 50% compared to arrival times based on picking the peak amplitude arrival (Figure 5). As expected, model amplitude decreases with increasing epicentral distance, but we find no systematic variation of growth or decay time with epicentral distance or water depth of the receiver (although note that there is limited range of both depth and distance). Because there is no systematic trend and there are trade-offs or covariance in the inversion between growth time, decay time and arrival time, we try fixing the growth and decay times to the average value of all the seismograms. Eliminating the trade-off in arrival time with other factors by fixing the shape in this way yields a further reduction in variance of nearly 50%, for an overall reduction of nearly 75% compared to picking the peak arrival time. Clearly, fitting a functional form to the envelope yields much more stable arrival time picks that should significantly improve estimates of epicentral location based on T-phases.

Further improvement would be possible if the variability in waveforms at individual stations could be predicted. The potential for improvement can be demonstrated by a comparative or relative event study of closed spaced events. We use an earthquake sequence at the northern end of the Easter microplate, consisting of a series of foreshocks and aftershocks; really an earthquake swarm rather than a mainshock sequence. Here we just describe results from the largest or mainshock and two of the aftershocks. Using the fixed-shape approach to picking arrival times, we find arrival times for each event. In addition to picking times at the ocean-bottom seismometer stations, we also pick arrivals at GSN station RPN, which is a similar distance away to the southeast (Figure 1). Taking the time difference between different events at the same station, we find differential times that are used to find relative event locations of the aftershocks relative to the mainshock. The variance from residuals of the relative event locations is much smaller than the travel-time residuals (Figure 5), indicating that there are systematic variations in waveform that are characteristic of particular stations and paths.

The relative event locations using T-phases show epicenters located up to about 30 km apart (Figure 6). This separation is larger than would normally be expected for a swarm on a mid-ocean ridge, calling into question the reliability of these locations. Some investigators have suggested, for example, that particular bathymetric features dominate the T-phase excitation. Could different features affect the excitation for different events in the same general source area, leading to biases in location? To test the precision of location, we have also performed relative event locations using Rayleigh and Love waves observed at teleseismic stations. We use a method of cross-correlating waveforms, employing phase velocities for young seafloor from Nishimura and Forsyth (1989) as the characteristic velocities in the source region for the calculation of locations. Waveforms from different events in the sequence are very similar (see for example, Figures 7 and 8), indicating that the mechanisms and depths are similar. There is a good azimuthal distribution of stations with adequate signal-to-noise ratio (Figure 9), yielding very precise relative locations.

The surface wave locations of these (Figure 6) and other events of the sequence show two sets of events distributed along nearly east-west lines, in accord with the strike of the fracture zones in this area and the left-lateral, strike-slip mechanism of the events inferred from the surface wave radiation patterns. The important point for this study is that the 95% confidence estimates for the locations using T-phases overlaps that of the

surface waves, indicating that there is no apparent bias in T-phase locations based on fitting shape functions to the entire envelope of the signal.

CONCLUSIONS

Fitting a functional shape to the log of the envelope of the T-phase greatly improves the picking of the arrival time compared to simply picking the time of peak energy. In addition, this approach uses the entire signal and is less likely to be influenced by individual bathymetric features affecting the excitation of the hydroacoustic phase. Relative event locations of a mainshock/aftershock sequence using surface waves confirms that there is no apparent bias in relative locations based on T-phases.

REFERENCE

Nishimura, C. E. and D. W. Forsyth (1989), The anisotropic structure of the upper mantle in the Pacific, Geophys. J., **96**, 203-229, 1989.

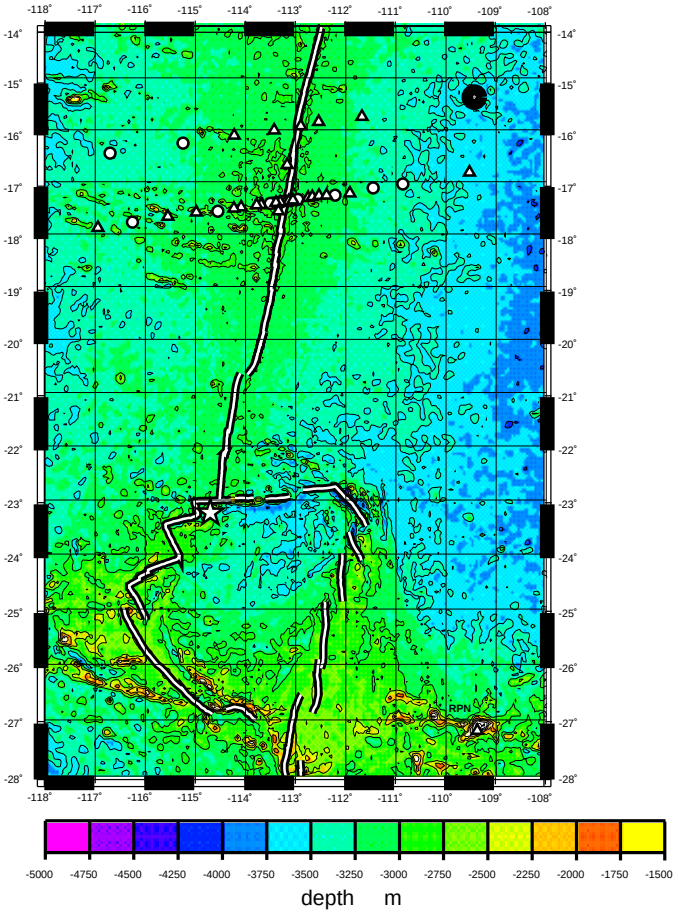

Figure 1. MELT Experiment location. Triangles represent ocean-bottom seismometers (OBS) equipped with 3-component seismometers as well as either hydrophones or differential pressure gauges. GSN station RPN shown in lower righthand corner. Star indicates location of earthquake sequence.

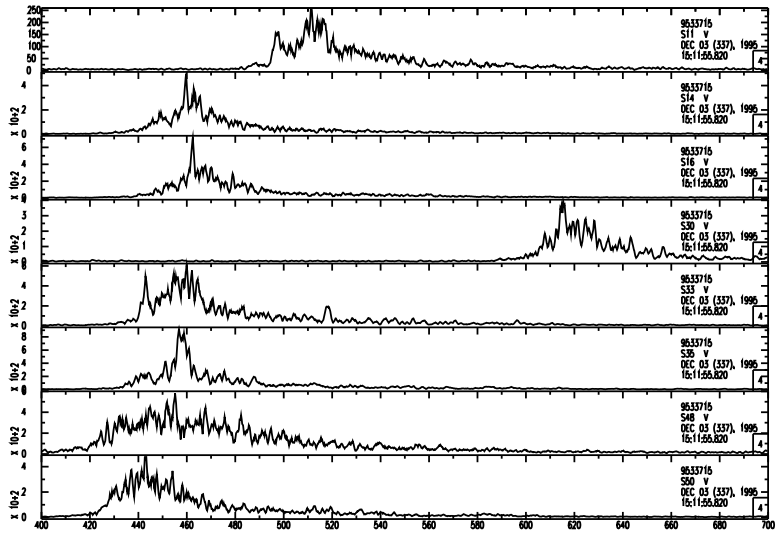

Figure 2. Smoothed envelopes of T phases recorded at several of the stations of the MELT array. These are vertical components, filtered 2 to 6 Hz.

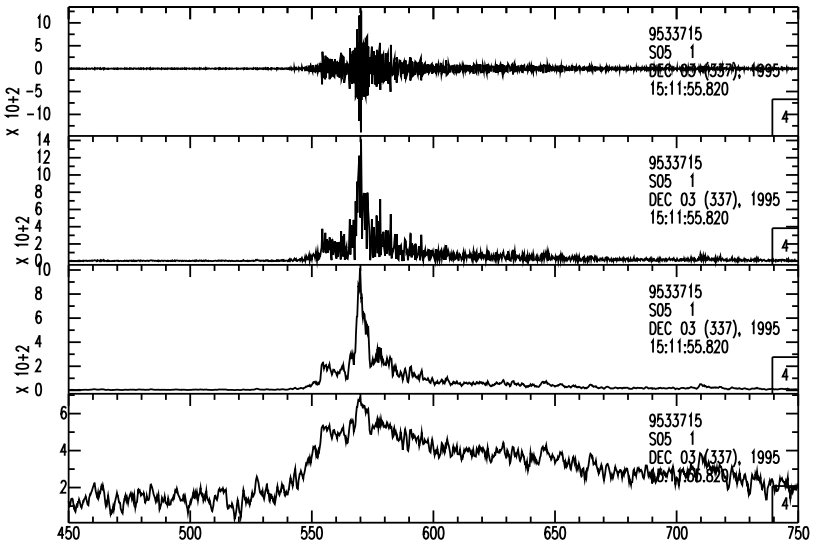

Figure 3. T-phase amplitude, envelope, smoothed envelope, and smoothed log envelope, from top to bottom. Noise is approximately log normal.

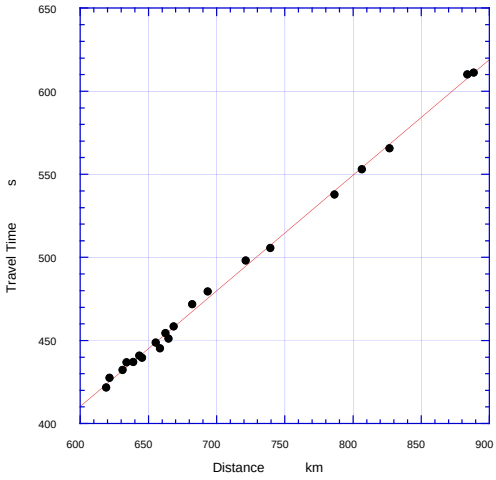

Figure 4. Travel time of T phase versus distance from the epicenter.

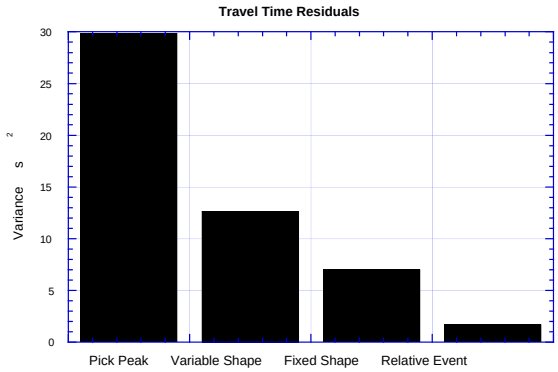

Figure 5. Variances of travel-time residuals estimated for four different approaches to picking arrival times.

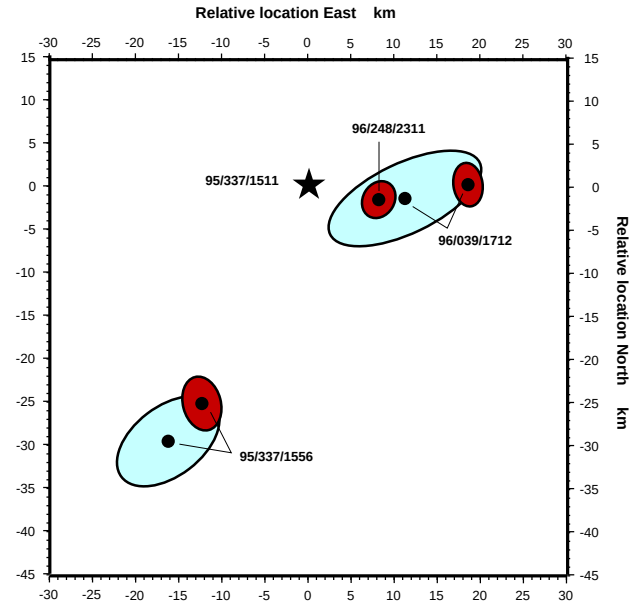

Figure 6. Locations of events relative to mainshock (star). Blue ellipses show 95% confidence ellipses from T phase relocations, red ellipses 95% limits from surface waves. Largest aftershock is located about 30 km to the SSE of mainshock on a parallel fracture zone. There is no apparent bias in T-phase locations based on fitting shape functions to the entire signal.

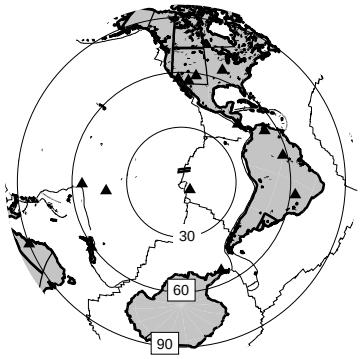

Figure 9. Azimuthal equidistant projection showing distribution of GSN stations (triangles) employed in relative event, surface wave location. Azimuthal coverage is good, with at least one station in every quadrant, i.e., better than the azimuthal distribution of stations recording T phases.

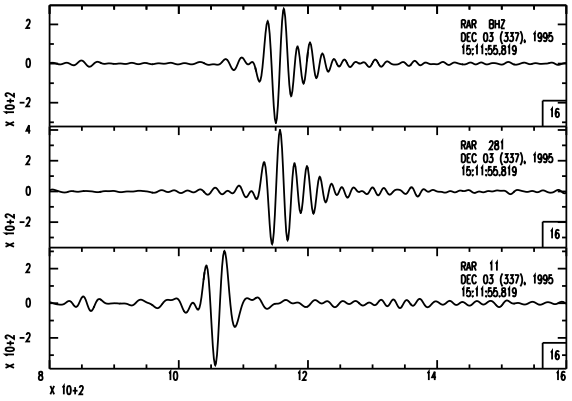

Figure 7. To corroborate relative event locations using T-phases, we use relative event locations determined from surface waves. These panels show vertical, radial, and transverse components, filtered from .02 to .05 Hz, recorded at GSN station RAR in French Polynesia at a distance of about 2800 km from the mainshock.

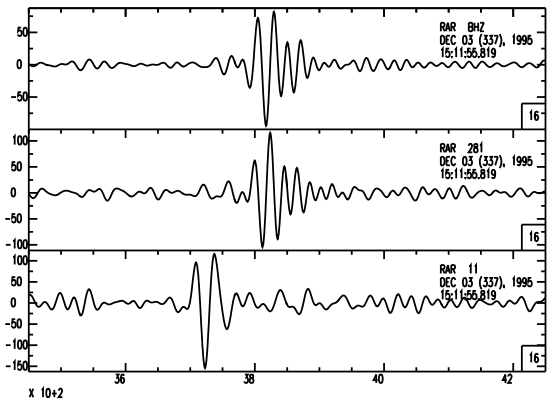

Figure 8. Vertical, radial and transverse components of the largest aftershock recorded at RAR, filtered from .02 to .05 Hz. Both Love and Rayleigh waves are used in the relocation. Note similarity of waveforms to the mainshock, despite differences in amplitude and location.